Highly-resonant two-polarization transmission guided-mode resonance filter

Léopold Macé, Olivier Gauthier-Lafaye, Antoine Monmayrant, Stéphane Calvez, Henri Camon, Hervé Leplan

Highly-resonant two-polarization transmission guided-mode resonance filter

Léopold Macé, Olivier Gauthier-Lafaye, Antoine Monmayrant, Stéphane Calvez, Henri Camon, and Hervé Leplan

View Online   Export Citation   CrossMark

ARTICLES YOU MAY BE INTERESTED IN

Highly-resonant two-polarization transmission guided-mode resonance filter

Léopold Macé,[1,2,a] Olivier Gauthier-Lafaye,[2] Antoine Monmayrant,[2] Stéphane Calvez,[2] Henri Camon,[2] and Hervé Leplan[1]

[1]*SAFRAN REOSC, Avenue de la Tour Maury, 91280 Saint-Pierre-du-Perray, France*
[2]*LAAS-CNRS, Université de Toulouse, CNRS, 31400 Toulouse, France*

We theoretically demonstrate a mid-infrared polarization-independent guided-mode-resonance transmission filter. We designed a structure based on a deeply-etched 2D grating above a thin slab of the same material respectively supporting transverse magnetic and transverse electric fundamental modes with identical effective index, which propagate along orthogonal directions. This device relates to multi-resonant guided-mode-resonance filters, and more particularly to the concept of zero-contrast gratings (ZCG), which can operate either as wideband reflectors [R. Magnusson, Optics Letters **39**, 4337 (2014)] or bandpass filters [M. Niraula, J. W. Yoon, and R. Magnusson, Optics Letters **40**, 5062 (2015)]. However, contrary to the latter, this new generation of filters is not bound by stringent material requirements inherent to conventional ZCGs. In particular, ZCGs are demonstrated with high to low refractive index ratio below 2, using germanium as high-index material over a low-index zinc sulfide substrate. These filters exhibit a transmission peak with a full-width at half-maximum of about 30 pm, and a maximum transmission close to 100 % lying in a 46-nm-wide rejection window. © *2018 Author(s). All article content, except where otherwise noted, is licensed under a Creative Commons Attribution (CC BY) license (http://creativecommons.org/licenses/by/4.0/).* https://doi.org/10.1063/1.5051621

I. INTRODUCTION

Our goal is to design polarization-insensitive transmission filters in the mid-IR range, between 3 and 4 μm, whose central wavelength could be easily varied for adjacent filters in a matrix. Zero-contrast gratings (ZCGs) have proven to be interesting solutions for the design of such filters: tunability of the resonance, few layers, planar structuration approach. Their principle, as described in Ref. 1, is to excite two distinct guided modes through two different grating orders in a single high-index partially-etched layer. These 2 orders differ in coupling strength, resulting in two *interfering/overlapping* Fano resonances with different widths. By placing the resonant peak of the narrowband resonance in the middle of the low transmission band of the broader one, an efficient transmission filter with a broad rejection band can be obtained. ZCG can operate either as wideband reflectors[2] or bandpass filters.[3] Besides, such narrowband 1D ZCGs can easily be implemented as 2D transmission filters with a simple parametric optimization.[4]

Another concept to design transmission filters in the long-IR range (8 − 14 μm)[5] relies on a high-contrast-grating (*HCG*) structure[6] that provides the broad rejection band.

The narrowband transmission resonance is obtained by breaking the in-plane symmetry of the system: either by using an off-normal incident plane wave,[5] or by introducing an asymmetry in the grating profile.[7,8] The difference in the coupling efficiency between the resonances responsible for the broad rejection band and the high-Q one originates from a variation in the overlap between the guided-modes and the incident plane wave. Depending on the polarization of the incident light and

---

[a]leopold.mace@laas.fr

     8, 115228-1

the orientation of the incident $\vec{k}$ vector, *TE* or *TM* resonances can appear. However, it is likely that polarization-insensitive devices based on these structures will prove quite challenging to design and fabricate. Therefore, we choose to develop a concept based on ZCG-like designs functioning under normal incidence rather than symmetry-related devices.

All ZCGs applied for filtering applications in the litterature exploit transverse electric (*TE*) guided-modes,[3,4,9,10] and will therefore be referred to as "pure *TE* ZCGs". Pure *TE* ZCGs get the required narrow- and large-band Fano resonances by coupling two guided modes through two different orders of the same grating: e.g. by coupling the fundamental TE_0 mode through the second grating order, and the TE_1 mode through the first grating order. Pure *TE* ZCGs thus need to support 2 modes with effective indices in a ratio of 2: the high-index layer supporting the guided-modes must have an index at least twice that of the low-index substrate.[1]

In a previous study,[11] we demonstrated 1D narrowband filters in the mid-IR based on pure *TE* ZCG. Besides, we presented a method to extend both angular acceptance and resonance width by more than a decade for 1D pure *TE* ZCG filters using a double-corrugation scheme for the grating. However, we didn't manage to extend this concept to a polarization-insensitive filter. Indeed, as we switch from a 1D to a 2D grating, many more grating orders as well as transverse magnetic (*TM*) modes need to be taken into account and prevented us from easily obtaining an efficient filter with a single transmission peak.

The above-described filters require a high-index contrast between the guiding layers and the embedding materials. From a practical point of vue, this condition is very limiting in the considered mid-IR range. Indeed, there are very few low-index substrates with low enough absorption in this spectral domain that can fulfill this condition, even with germanium ($n \approx 4.15$) as high-index material. The most appropriate ones are fluorides,[12] which are expensive, fragile, and hygroscopic.

A slightly different approach has been recently demonstrated.[13] Instead of relying on 2 guided modes of a single waveguide coupled by 2 orders of a single grating to generate 1 large and 1 narrow Fano resonances, this method uses 2 single-mode waveguides and a 2D grating for polarization independence. The waveguide closest to the grating provides the large Fano resonance (strong coupling), while the further provides the narrow Fano resonance (weak coupling). Contrary to single-layer multimodal waveguides, the fundamental modes in the two isolated waveguides can have their effective index adjusted independently. When the 2D grating is a hole-type (resp.rod-type) photonic crystal, then, the device is shown to couple two *TE* (resp. *TM*) guided-modes. It shows that both kinds of modes can be used to design bandpass filters.

In this article, we present an original approach for the design of transmission filters that combines the flexibility of the two-waveguide approach with the simplicity of the partially-etched single-layer designs. We design a ZCG that supports *TE* and *TM* fundamental modes with identical effective index, propagating along orthogonal directions, which we will call "*TE/TM* ZCGs". We use a deeply-etched 2D grating above a thin slab of the same material, which is designed such that the *TE* mode is mostly guided in the slab, while the *TM* one lies within the ridges of the grating (see Fig. 1). Because these modes are confined within separate parts of the high-index structure, their effective index can be tuned almost independently. This method allows us to couple guided-modes with close effective index, thereby relieving the stringent condition on the refractive index of the materials while using a simple, partially-etched, single-layer structure. The resulting filters are intrinsically polarization-insensitive and benefit from the tunability of guided-mode resonance filters.
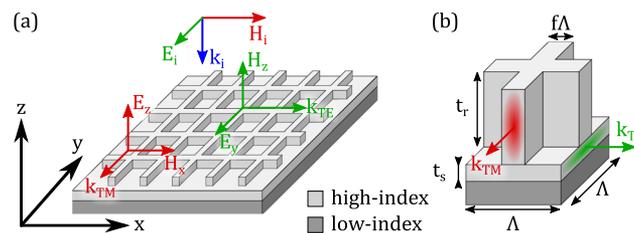

FIG. 1. (a) Schematics of the 2D square-lattice structure illustrating the orthogonal phase propagation directions of the coupled *TE* and *TM* guided-modes. (b) Naming convention.

II. DESIGN

We use germanium (Ge) as waveguide material and calcium fluoride (CaF$_2$) as substrate. Indeed, these materials are highly transparent in midIR range, which makes them very appropriate for transmission filters. Moreover, we want to show that we can achieve performance equivalent to that of purely *TE* ZCGs that require such materials.[11] The structure is composed of a slab waveguide above which lies a square grating of the same material with ridges along the $x-$ and $y-axis$ (see Fig. 1). For symmetry reasons, polarization independence under normal incidence is immediate for such a device.[14,15] Therefore, we can consider only one polarization state of light, for example $E = E_y$ and $H = H_x$. The starting idea is schematically described in Fig. 1(a): we want to design a filter using two resonances originating from the coupling of one *TE* and one *TM* mode propagating in orthogonal directions. The *TE* mode is mainly guided in the slab, while the *TM* one is confined within the deep grating ridge (see Fig. 1(b)). These modes possess similar yet independently tunable effective indices, and have widely different overlaps with the grating, thus resulting in a large Fano resonance (*TE* mode) and a narrow one (*TM* mode) in the same wavelength range.

In order to obtain a single transmission peak, we want to limit the number of guided modes and coupling orders. Ideally, we thus want to have one single *TM* mode and one single *TE* mode in the whole structure and couple them through the first grating order. However, it is not possible to match the indices of the TE_0 and TM_0 modes in a slab waveguide. Thus, we choose to use a high aspect-ratio grating.

By doing so, we keep the waveguide thin enough to support only the fundamental *TE* mode, while the high grating ridges should support a fundamental *TM* mode of close effective index. The indices of the modes can then be tuned almost independently, by changing slightly either the ridge height t_r or the slab thickness t_s. We thus have the same flexibility as with two separated waveguides.[13]

A. Waveguide design

The starting point is a Ge slab waveguide above a CaF$_2$ substrate. In the following we use for the Ge refractive indices data extracted by ellipsometry on sputtered thin films, and on manufacturer's data for the CaF$_2$ substrate.[16]

We choose a slab waveguide thickness $t_s = 0.22\ \mu m$. For this value, and at $\lambda = 3.5\ \mu m$: $n_{TE_0}^{slab} = 2.67$. Let us note that the fundamental *TM* mode is also present, but with $n_{TM_0}^{slab} = 1.42 \neq 2.67$. Since its index is significantly lower than that of the *TE* mode, it won't result in a resonance close to that arising from the coupling of the fundamental *TE* mode and can safely be ignored. For the rest of the study we can consider that the slab only supports the fundamental *TE* mode hereafter called the slab mode or *TE* mode.

B. Grating design

The next step consists in adding the deep ridge grating that will support a *TM* mode, hereafter called the ridge mode or *TM* mode. The first condition is that the grating should couple to free space the *TE* slab mode through the first order. We use the phase matching condition given in Ref. 1 to determine the period Λ ensuring a resonant coupling of the *TE* slab mode around $\lambda = 3.5\ \mu m$:

$$\Lambda = \lambda / n_{TE_0}^{slab} \simeq 1.255\ \mu\text{m} \tag{1}$$

This parameter is not crucial, since the period is a tunable parameter that will allow us to eventually tune the central wavelength of the filter. Besides, as the grating ridges height increases, the effective index of the slab *TE* mode increases. The grating ridge fillfactor is chosen close to $f = 0.26$, which is small enough to limit the coupling between *TM* modes in adjacent ridges, but also high enough to keep a reasonable aspect ratio in order to ensure the fabricability of the structure. Fig. 2(a) shows the dispersion of the slab *TE* (red curve) and ridge *TM* (green curve) modes in the structure as a function of the grating ridge height t_r (see Fig. 1(b)), together with the H-field principal component for each mode namely H_x for the *TM* mode (Fig. 2(b)) and H_z for the *TE* mode (Fig. 2(c)). The calculation is performed for a single grating ridge on an infinite slab waveguide using an optical eigenmode solver for dielectric waveguides.[17] The grating is considered as a one-dimensional structure, therefore both modes are given in the (Oxz) plane. The lateral and
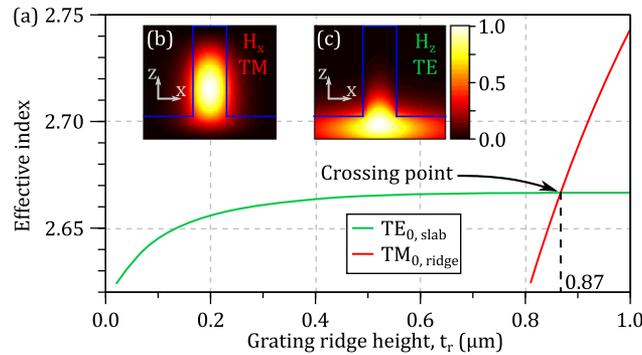
FIG. 2. (a) Effective index for the *TE* (green curve) and *TM* (red curve) modes as a function of the ridge height t_r. In (b) and (c) are respectively given the square amplitude of the x and z components of the magnetic field within a period of the filter for $t_r = 0.87 \, \mu m$ (crossing point of the dispersion curves). The calculation is performed at $\lambda = 3.6179 \, \mu m$. At this wavelength, the material indices are: $n_{Ge} = 4.173$ and $n_{CaF_2} = 1.413$. The fixed dimensions are as follows: $t_s = 0.22 \, \mu m$, $\Lambda = 1.255 \, \mu m$ and $f\Lambda = 321.3 \, nm$.

vertical extension of the simulation domain as well as the mesh resolution are sufficient to ensure convergence.

We can see in Fig. 2(a) that the dispersion curves of both modes cross for $t_r = 0.87 \, \mu m$. In the vicinity of this point, the effective index of the *TM* mode (Fig. 2(a), red curve) is largely affected by the ridge height t_r, while that of the *TE* mode (Fig. 2(a), green curve) barely varies. This is due to the fact that the *TM* mode is mainly confined in the ridge, while the *TE* mode is mainly confined in the slab, as shown on Figs. 2(b) and 2(c). As a consequence the ridge and slab modes can be tuned almost independently: the grating ridge height t_r controls the *TM* ridge mode effective index, while the slab waveguide thickness mainly determines that of the *TE* slab mode.

C. Parametric study

The crossing point determined above (see Fig. 2(a)) is only a starting point for an optimization procedure conducted with the *S4* code,[18] which uses RCWA and the S-matrix algorithm. The filter transmission map $T(\lambda, t_r)$ is shown in Fig. 3. This RCWA simulation is performed using 121 harmonics. The region in the vicinity of $t_r = 0.99 \, \mu m$ and $\lambda = 3.62 \, \mu m$ is of particular interest to us. Indeed, a single high-transmission resonance lies within a broad rejection band.

The transmission of the filter with a ridge height of $t_r = 0.99 \, \mu m$ (corresponding to the light blue line in Fig. 3) is plotted in Fig. 4. A higher number of harmonics (501) is used to ensure full convergence of the solution, in order to resolve the narrow spectral peak. Fig. 4(a) shows a high-transmission peak around $\lambda = 3.624 \, \mu m$, having a FWHM of 30 pm within a 46 nm-wide rejection
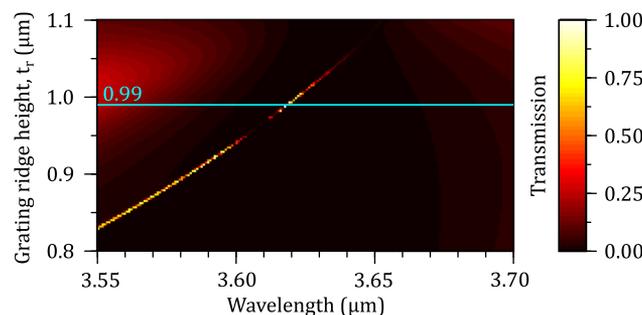

FIG. 3. Transmission spectrum as a function of the grating ridge height t_g. The light blue line corresponds to the case $t_r = 0.99 \, \mu m$, taken as reference for the rest of the study. The fixed device parameters are as follows: $t_s = 0.22 \, \mu m$, $\Lambda = 1.255 \, \mu m$ and $f\Lambda = 321.3 \, nm$.
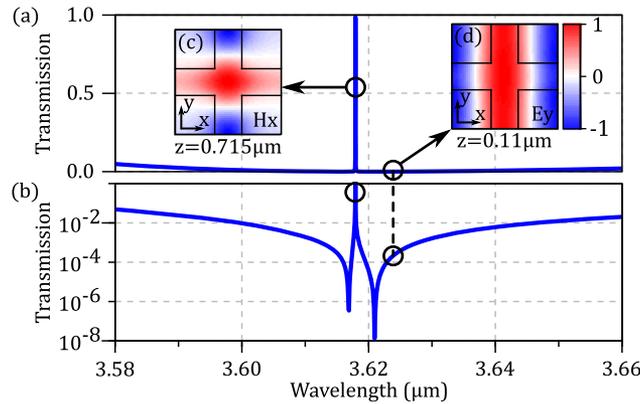
FIG. 4. Transmission spectra for a particular highly-resonant filter using a Ge partially etched-grating above a CaF$_2$ substrate shown on both (a) linear and (b) logarithmic scales. The insets in a) show the real part of the most significant components of the electric and magnetic fields within one period of the (Oxy) plane of the structure on an orthonormal scale at particular z values. In (c) is given the H_x field for $z = 0.715$ μm calculated at the resonance wavelength $\lambda_{res} = 3.6179$ μm, while in (d) is presented the E_y field at $z = 0.11$ μm within the rejection band ($\lambda = 3.624$ μm). The dimensions are as follows: $t_s = 0.22$ μm, $t_r = 0.99$ μm, $\Lambda = 1.255$ μm et $f\Lambda = 321.3$ nm.

band of $T < 1\%$. In Fig. 4(b), we can see that the transmission peak is flanked by 2 high-rejection dips, which means that there are indeed two Fano resonances in the system.

Our aim is to identify the particular couplings occurring here. For this, we calculate the electric and magnetic fields within one period of the (Oxy) plane of the structure in the middle of the slab and ridge heights.

At the resonant peak, the most intense component of the fields are H_x (shown in Fig. 4(c)) and E_z (not shown) within the middle of the ridge. This confirms that the guided mode responsible for this narrow resonance is a *TM* mode, confined in the ridge. Moreover, the inspection of the isovalues in Fig. 4(c), shows that this mode propagates in the ridge along the y direction.

On the contrary, within the broad rejection band, the most intense components of the fields are H_z (not shown) and E_y (shown in Fig. 4(d)) and they are confined in the middle of the slab. The rejection band is thus due to the coupling with a *TE* mode, that propagates along the x direction, as can be deduced from Fig. 4(d).

Our ZCG filter is thus relying on the coupling of one *TE* and one *TM* mode, propagating along orthogonal directions, as was depicted in Fig. 1(a). Furthermore, Figs. 4(c) and 4(d) show that the coupled modes have the same periodicity than the coupling grating, confirming that the resonances arise from first-order couplings.

Fig. 4 demonstrates a new filter design which, for the first time, simultaneously uses a *TE* and a *TM* resonance to respectively provide the broad resonance band and high-transmission peak of a single-layer photonic structure. In this regard, it significantly differs from pure *TE* ZCGs that rely only on *TE* modes. The main advantage of our approach is that it relies on eigenmodes with similar indices (see Fig. 2) coupled by the same first grating order (see Figs. 4(c) and 4(d)). As a consequence and contrarily to pure *TE* ZCGs, it is not limited by the stringent condition that the partially-etched high-index layer should have an index larger than twice that of the substrate.[1] Indeed, the sole restriction in our approach is a higher index than that of the substrate, like any conventional waveguide.

To demonstrate this significant difference, we have designed another *TE/TM* ZCG with a Ge layer ontop of ZnS substrate that has a significantly higher refractive index than the CaF$_2$ substrate used previously. The change in design related to the change in substrate from CaF$_2$ (see dimensions listed in the caption of Fig. 4) to higher-index ZnS (caption of Fig. 5) is quite straightforward. The thickness, t_s, of the slab waveguide layer should be decreased in order to compensate for the increase in the *TE* mode effective index. The *TM* mode, which is confined within the grating ridge is barely affected by the substrate, and therefore we only perform a slight optimization of the grating ridge. The lateral dimensions are thus identical to that of the previous design (see Fig. 4).
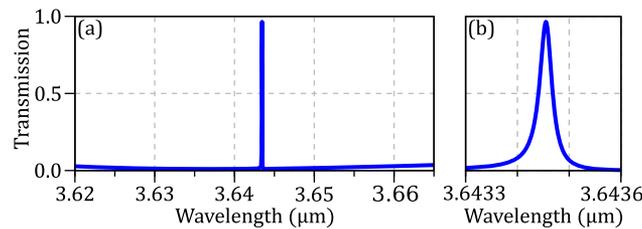
FIG. 5. (a) Transmission spectrum for a particular highly-resonant filter using *Ge* slab and grating above a *ZnS* substrate, with (b) a zoom in the vicinity of the transmission peak. At the resonance wavelength of the transmission peak ($\lambda = 3.6435 \ \mu m$): $n_{Ge} = 4.173$ et $n_{ZnS} = 2.164$. The dimensions of the filter are the following ones: $t_s = 0.198 \ \mu m$, $t_r = 1.02 \ \mu m$, $\Lambda = 1.255 \ \mu m$ and $f\Lambda = 321.3 \ nm$.

Fig. 5 shows the transmission curve of this new filter, calculated by RCWA, using 501 harmonics. The resonance wavelength of this device is $\lambda = 3.6435 \ \mu m$, for which the indices of the Ge and ZnS are respectively of $n_{Ge} = 4.173$ and $n_{ZnS} = 2.16$, in a ratio of $n_{Ge}/n_{ZnS} \simeq 1.93 < 2$. Our approach of *TE/TM* ZCGs thus extends ZCGs to a wider range of materials with lower refractive index contrast.

D. Conclusion

A new approach for the design of ZCG filters, *TE/TM*-ZCGs has been proposed and numerically demonstrated. Contrary to pure *TE* ZCGs reported so far, it relies on a 2D deep-ridge grating which simultaneously couples one fundamental *TE* and one fundamental *TM* modes which exhibit similar effective indexes and whose propagation occurs along orthogonal directions. It differs from pure *TE* ZCGs in two ways. First, contrary to pure *TE* ZCGs that can be designed as 1D structures, *TE/TM*-ZCGs are inherently 2D structures providing polarization independence under normal incidence. Second, *TE/TM*-ZCGs can be designed on a wider range of material systems as they do not require a high index material with a refractive index at least twice higher than that of the underlying substrate. This approach was successfully used to design several narrowband transmission filters in the midIR, with different substrate materials.

ACKNOWLEDGMENTS

[1] Y. Ding and R. Magnusson, "Doubly resonant single-layer bandpass optical filters," Optics Letters **29**, 1135–1137 (2014).

[2] R. Magnusson, "Wideband reflectors with zero-contrast gratings," Optics Letters **39**, 4337 (2014).

[3] M. Niraula, J. W. Yoon, and R. Magnusson, "Single-layer optical bandpass filter technology," Optics Letters **40**, 5062 (2015).

[4] Y. H. Ko and R. Magnusson, "Flat-top bandpass filters enabled by cascaded resonant gratings," Optics Letters **41**, 4704 (2016).

[5] J. M. Foley, S. M. Young, and J. D. Phillips, "Symmetry-protected mode coupling near normal incidence for narrow-band transmission filtering in a dielectric grating," Physical Review B **89** (2014).

[6] V. Karagodsky and C. J. Chang-Hasnain, "Physics of near-wavelength high contrast gratings," Optics Express **20**, 10888–10895 (2012).

[7] J. M. Foley and J. D. Phillips, "Normal incidence narrowband transmission filtering capabilities using symmetry-protected modes of a subwavelength, dielectric grating," Optics Letters **40**, 2637 (2015).

[8] X. Cui, H. Tian, Y. Du, G. Shi, and Z. Zhou, "Normal incidence filters using symmetry-protected modes in dielectric subwavelength gratings," Scientific Reports **6** (2016).

[9] M. Niraula, J. W. Yoon, and R. Magnusson, "Mode-coupling mechanisms of resonant transmission filters," Optics Express **22**, 25817 (2014).

[10] M. Niraula, J. W. Yoon, and R. Magnusson, "Concurrent spatial and spectral filtering by resonant nanogratings," Optics Express **23**, 23428 (2015).

[11] L. Mac, O. Gauthier-Lafaye, A. Monmayrant, and H. Camon, "Design of angularly tolerant zero-contrast grating filters for pixelated filtering in the mid-IR range," Journal of the Optical Society of America A **34**, 657 (2017).

[12] P. Yeh, *Optical waves in layered media* (Wiley, 2005).

[13] S.-G. Lee, S.-H. Kim, K.-J. Kim, and C.-S. Kee, "Polarization-independent electromagnetically induced transparency-like transmission in coupled guided-mode resonance structures," Applied Physics Letters **110**, 111106 (2017).

[14] S. Peng and G. M. Morris, "Resonant scattering from two-dimensional gratings," Journal of the Optical Society of America A **13**, 993 (1996).

[15] A.-L. Fehrembach, D. Maystre, and A. Sentenac, "Phenomenological theory of filtering by resonant dielectric gratings," JOSA A **19**, 1136–1144 (2002).

[16] Crystran Ltd, "Calcium fluoride,".

[17] A. B. Fallahkhair, K. S. Li, and T. E. Murphy, "Vector finite difference modesolver for anisotropic dielectric waveguides," Journal of Lightwave Technology **26**, 1423–1431 (2008).

[18] V. Liu and S. Fan, "S4: A free electromagnetic solver for layered periodic structures," Computer Physics Communications **183**, 2233–2244 (2012).